Available online at www.sciencedirect.com
ScienceDirect
Atmospheric Environment 42 (2008) 3076–3086
ATMOSPHERIC ENVIRONMENT
www.elsevier.com/locate/atmosenv

Scavenging of soluble gases by evaporating and growing cloud droplets in the presence of aqueous-phase dissociation reaction

Tov Elperin*, Andrew Fominykh, Boris Krasovitov

Department of Mechanical Engineering, The Pearlstone Center for Aeronautical Engineering Studies, Ben-Gurion University of the Negev, P.O. Box 653, Beer Sheva 84105, Israel

Received 11 September 2007; received in revised form 13 December 2007; accepted 13 December 2007

Abstract

In this study we performed numerical analysis of simultaneous heat and mass transfer during evaporation and condensation of a cloud droplet in the presence of soluble gases. It is assumed that gas absorption is accompanied by subsequent aqueous-phase equilibrium dissociation reactions. The system of transient conjugate nonlinear energy and mass conservation equations was solved using anelastic approximation and taking into account thermal effect of gas absorption. It was shown that nonlinear behavior of different parameters, such as temperature and absorbate concentration at the droplet surface stems from the interaction of heat and mass transfer processes. We found that thermal effect of absorption and Stefan flow result in the maximum of droplet surface temperature during the transient period of droplet evaporation. It was shown that heat and mass transfer rates in water droplet–air–water vapor system at short times are considerably enhanced under the effects of Stefan flow, heat of absorption and dissociation reactions within the droplet. Comparison of the results obtained using the model of physical absorption of sulfur dioxide in water droplet with the predictions of the present model that takes into account the subsequent equilibrium dissociation reactions showed that the model of physical absorption underestimates the value of droplet surface temperature and overestimates the average concentration of $[SO_2 \cdot H_2O]$ at the transient stage of gas absorption. The performed calculations showed that the value of pH increase with the increasing relative humidity (RH).

Keywords: Heat transfer; Mass transfer; Droplet evaporation; Gas absorption

1. Introduction

Clouds play an important role in removing gaseous pollutants from atmosphere. Scavenging of atmospheric gaseous pollutants by cloud droplets is a result of gas absorption mechanism (Pruppacher and Klett, 1997; Flossmann, 1998). Presence of soluble gas in the atmosphere can affect the dynamics of evaporation and condensation of water droplets in the atmospheric clouds. Comprehensive study of coupled heat and mass transfer during gas absorption by liquid droplets and droplets evaporation and growth is a necessary step for adequate predicting of atmospheric changes under the influence of hazardous gases.

Gas absorption by non-evaporating droplets accompanied by subsequent dissociation was discussed by Baboolal et al. (1981), Walcek and

*Corresponding author. Tel.: +972 8 6477078; fax: +972 8 6472813.
E-mail address: elperin@bgu.ac.il (T. Elperin).

1352-2310/$ - see front matter © 2007 Elsevier Ltd. All rights reserved.
doi:10.1016/j.atmosenv.2007.12.036

Nomenclature

c_p	specific heat at a constant pressure ($J\,kg^{-1}\,K^{-1}$)
D_j	diffusion coefficient of jth species in the gaseous phase ($m^2\,s^{-1}$)
D_{jk}	binary diffusion coefficient in the gaseous phase ($m^2\,s^{-1}$)
K_h	Henry's constant ($mol\,m^{-3}\,Pa^{-1}$)
K_1, K_2	equilibrium constants ($mol\,m^{-3}$)
k	thermal conductivity ($W\,m^{-1}\,K^{-1}$)
L_v	latent heat of evaporation ($J\,kg^{-1}$)
L_a	heat of dissolution ($J\,kg^{-1}$)
M_j	molar mass of jth species ($kg\,mol^{-1}$)
m_L	mass of the droplet (kg)
p	pressure (Pa)
r	radial coordinate (m)
R	radius of the droplet (m)
R_g	universal gas constant ($J\,mol^{-1}\,K^{-1}$)
RH	relative humidity
T	temperature (K)
t	time (s)
v	velocity ($m\,s^{-1}$)
V_d	droplet volume (m^3)
Y	mass fraction

Greek symbols

ρ	density ($kg\,m^{-3}$)
τ	dimensionless time

Subscripts and superscripts

0	initial value
1	volatile species
A	absorbate
e	value outside a droplet
j	number of a species
L, (L)	liquid
s	value at the droplet surface
∞	value at infinity

Pruppacher (1984), Walcek et al. (1984), Waltrop et al. (1991), Mitra and Hannemann (1993), Saboni and Alexandrova (2001), Alexandrova et al. (2004). The observations show that in atmospheric clouds and rain water the pH ($pH = -\log[H^+]$) is typically in the range from 3 to 6. Mitra and Hannemann (1993), Saboni and Alexandrova (2001), Alexandrova et al. (2004) investigated theoretically mass transfer during SO_2 absorption by water droplets for $pH \leqslant 5.5$ neglecting formation of sulphite (SO_3^{2-}). Formation of SO_3^{2-} was discussed by Baboolal et al. (1981) and Walcek and Pruppacher (1984). Huckaby and Ray (1989) developed a model which takes into account formation of SO_3^{2-} ions during sulfur dioxide absorption by water droplets. All the above studies assume local chemical equilibrium between the gaseous and liquid phases during SO_2 absorption by water droplets. Assumption of local chemical equilibrium is based on the examining relaxation times of the SO_2 hydrolysis and ionization equilibria, time required for attaining local phase equilibrium at gas–liquid interface (SO_2(g)/water) and characteristic time of diffusion in a droplet (see Schwartz and Freiberg, 1981; Gardner et al., 1987).

Ray et al. (1987) and Huckaby and Ray (1989) investigated theoretically an influence of vapor condensation at the surface of stagnant droplets on the rate of mass transfer during gas absorption by growing droplets. Ray et al. (1987) analyzed gas absorption by a stationary growing droplet in a stagnant supersaturated medium by solving the coupled non-stationary mass and energy balance equations for the gaseous and liquid phases. The obtained results showed that in the case when heats of condensation are small the droplet growth can increase significantly the rate of absorption. Huckaby and Ray (1989) employed the approach suggested by Ray et al. (1987) to investigate a system consisting of a liquid droplet, its vapor, soluble and inert gases and took into account diffusion resistances in both phases during gas absorption. Numerical calculations were performed for water droplet evaporating/growing in gaseous mixture containing sulfur dioxide (SO_2).

The effect of evaporation on sulfur dioxide absorption/desorption of soluble gases by moving droplet was investigated by Marion et al. (2006). Liquid in a droplet was assumed to be fully mixed due to circulations caused by shear stress at gas–droplet interface. Concentration of soluble gas and temperature inside a droplet are uniform and time-dependent. In the model developed by Marion et al. (2006), the droplet radius was assumed to be constant. Using the mass and energy balance relations and empirical correlations for Sherwood

and Nusselt numbers Marion et al. (2006) determined droplet temperature and the absorption rate as functions of time. The obtained theoretical results were compared with the experimental data.

Note that Ray et al. (1987), Huckaby and Ray (1989) and Marion et al. (2006) investigated only the influence of evaporation (condensation) on the rate of gas absorption by liquid droplets. In the present study, we investigate the interrelated effects of gas absorption, evaporation/condensation and dissociation of the dissolved gas on transient heat and mass transfer in the presence of inert gases. We also take into account the following effects that have been neglected in all previous studies: (i) effect of gas absorption on Stefan velocity; (ii) effect of heat of absorption on droplet evaporation/condensation; (iii) droplet growth due to gas absorption. In distinction to previous studies (see e.g., Ray et al., 1987; Huckaby and Ray, 1989) in our calculations we consider the molecular transport coefficients of the gaseous phase as functions of temperature and concentrations of gaseous species. Consequently, the suggested model can be used over a wide range of parameters such as temperature, relative humidity and the concentration of soluble gas in a gaseous phase, etc.

2. Model description

2.1. Governing equations

Consider a spherical droplet with the initial radius R_0 immersed in a stagnant gaseous mixture with temperature $T_{e,\infty}$. The gaseous mixture contains non-condensable soluble species that is absorbed into the liquid. The first component of the gaseous mixture is formed by molecules of the volatile species of a droplet. The soluble species is absorbed into the liquid. Molecules of the other $K-2$ components do not penetrate inside the droplet. The droplet is heated by heat conduction from the surroundings and begins to evaporate. In further analysis, we assume spherical symmetry and neglect effects of buoyancy and thermal diffusion. Under these assumptions, the system of mass and energy conservation equations for the liquid phase $0<r<R(t)$ reads:

$$r^2\frac{\partial Y_{\rm A}^{(\rm L)}}{\partial t}=D_{\rm L}\frac{\partial}{\partial r}\left(r^2\frac{\partial Y_{\rm A}^{(\rm L)}}{\partial r}\right),\qquad r^2\frac{\partial T^{(\rm L)}}{\partial t}=\alpha_{\rm L}\frac{\partial}{\partial r}\left(r^2\frac{\partial T^{(\rm L)}}{\partial r}\right). \tag{1}$$

In the surrounding gaseous medium, $r>R(t)$, the mass, species and energy conservation equations read:

$$r^2\frac{\partial\rho}{\partial t}+\frac{\partial}{\partial r}(r^2\rho v_r)=0, \tag{2}$$

$$r^2\frac{\partial}{\partial t}(\rho Y_j)+\frac{\partial}{\partial r}(\rho v_r r^2 Y_j)=\frac{\partial}{\partial r}\left(\rho D_j r^2\frac{\partial Y_j}{\partial r}\right), \tag{3}$$

$$r^2\frac{\partial(\rho c_p T_e)}{\partial t}+\frac{\partial}{\partial r}(\rho v_r r^2 c_p T_e)=\frac{\partial}{\partial r}\left(k_e r^2\frac{\partial T_e}{\partial r}\right). \tag{4}$$

In Eqs. (1)–(4) ρ is the gas density, j is the number of gaseous phase species (subscript 1 denotes the volatile species, $j=1,\ \ldots,\ K-1, j\neq$A), Y_j is the mass fraction of the jth gaseous species, $Y_{\rm A}^{(\rm L)}$ is the mass fraction of the absorbate in the liquid, D_j is the diffusion coefficient, $D_j=(1-X_j)/\sum_{k\neq j}(X_k/D_{jk})$, X_j is the mole fraction of the jth species, D_{jk} is the binary diffusion coefficient for species j and k. Note that in general, Eq. (3) are written for all $j=1,\ \ldots,\ K$. However, only $K-1$ of the values D_j can be specified independently. Consequently, the Kth species can be treated differently from the others and may be found consistently using the identity

$$\sum_{j=1}^{K}Y_j=1.$$

When $v^2/c^2\ll 1$ (where v is the gas velocity and c is the speed of sound) instead of Eq. (2) anelastic approximation can be used

$$\frac{\partial}{\partial r}(r^2\rho v_r)=0. \tag{5}$$

The system of energy and mass conservation Eqs. (2)–(4) must be supplemented with the momentum conservation equation. However, in the case of subsonic flow velocities (low Mach number approximation, $M\ll 1$) the pressure gradient is negligibly small ($\Delta p\sim\rho v^2$) and, therefore, the pressure can be assumed constant. The gaseous phase properties can be related through the ideal gas equation of state:

$$p=p_\infty=\rho R_{\rm g}T_e\sum_{j=1}^{K}\left(\frac{Y_j}{M_j}\right). \tag{6}$$

where M_j is the molar mass of the jth gaseous species.

Eqs. (1)–(5) must be supplemented with equation for determining gas velocity. The exprressions for Stefan velocity and the rate of change of

droplet radius were obtained using the macroscopic mass balance at the droplet surface: $dm_L/dt = -4\pi R^2 \rho_s (v(R,t) - \dot{R})$. Following the approach developed by Elperin et al. (2007a) we obtain the following expressions for Stefan velocity and the rate of change of droplet radius:

$$v_s = -\frac{D_L \rho_L}{\rho(1-Y_1)} \frac{\partial Y_A^{(L)}}{\partial r}\bigg|_{r=R_-} - \frac{D_1}{(1-Y_1)} \frac{\partial Y_1}{\partial r}\bigg|_{r=R_+}, \tag{7}$$

$$\dot{R} = \frac{D_L}{1-Y_1} \frac{\partial Y_A^{(L)}}{\partial r}\bigg|_{r=R_-} + \frac{\rho D_1}{\rho_L (1-Y_1)} \frac{\partial Y_1}{\partial r}\bigg|_{r=R_+}, \tag{8}$$

where the signs "+" and "−" denote values at the external and internal surfaces, respectively, and ρ_L is the liquid density. The radial flow velocity v_r as a function of r and t can be obtained by integrating Eq. (5): $v_r = \rho_s v_s R^2/(\rho r^2)$, where v_s is determined from Eq. (7).

As can be seen from expressions (7) and (8), the absorption of soluble admixture causes the decrease of Stefan velocity and evaporation rate. However, since absorption is accompanied by thermal effect, reaction of dissociation and solubility of different gases in the same liquid differs essentially, the influence of gas absorption on the rate of evaporation is quite involved.

2.2. Initial and boundary conditions and aqueous-phase chemical equilibria

The system of conservation Eqs. (1)–(4) must be supplemented by initial conditions and the boundary conditions at the droplet surface. The initial conditions for the system of Eqs. (1)–(4) read:

$$\begin{aligned} &\text{At } t=0, \quad 0 \leqslant r \leqslant R_0, \quad T^{(L)} = T_0^{(L)}, \quad Y_A^{(L)} = Y_{A,0}^{(L)}, \\ &\text{At } t=0, \quad r \geqslant R_0, \quad T_e = T_{e,0}(r), \quad Y_j = Y_{j,0}(r). \end{aligned} \tag{9}$$

At the droplet surface the continuity conditions for the radial flux of non-soluble gaseous species yield:

$$D_j \rho \frac{\partial Y_j}{\partial r}\bigg|_{r=R_+} = \rho Y_j v_s. \tag{10}$$

For the absorbate, this condition assumes the form of the following equation (for details, see Elperin et al., 2007a):

$$j_A\big|_{r=R} = \rho Y_A v_s - D_A \rho \frac{\partial Y_A}{\partial r}\bigg|_{r=R_+} = -D_L \rho_L \frac{\partial Y_A^{(L)}}{\partial r}\bigg|_{r=R_-} \tag{11}$$

The vapor concentration at the droplet surface $Y_{1,s}$ is a function of temperature $T_s(t)$ and is determined as follows: $Y_{1,s}(T_s) = \rho_{1,s}/\rho = p_{1,s}(T_s) M_1/p_\infty M$, where $p_{1,s}$ is the partial pressure at the droplet surface.

The droplet temperature can be found from the following equation:

$$k_e \frac{\partial T_e}{\partial r}\bigg|_{r=R_+} + \rho_L L_v \frac{dR}{dt} = k_L \frac{\partial T^{(L)}}{\partial r}\bigg|_{r=R_-} - L_a \rho_L D_L \frac{\partial Y_A^{(L)}}{\partial r}\bigg|_{r=R_-} \tag{12}$$

The last term on the right-hand side of Eq. (12) arises due to a heat released at gas–liquid interface during gas absorption in liquid (see, e.g., Elperin and Fominykh, 2005; Elperin et al., 2007b). The following equilibrium reactions occur when SO_2 is dissolved in water droplet (see, e.g., Seinfeld, 1986):

$$SO_2(g) + H_2O \xrightarrow{K_h} SO_2 \cdot H_2O, \quad K_h = \frac{[SO_2 \cdot H_2O]}{p_{SO_2}}, \tag{13}$$

$$SO_2 \cdot H_2O \xrightarrow{K_1} H^+ + HSO_3^-, \quad K_1 = \frac{[H^+][HSO_3^-]}{[SO_2 \cdot H_2O]}, \tag{14}$$

$$HSO_3^- \xrightarrow{K_2} H^+ + SO_3^{2-}, \quad K_2 = \frac{[H^+][SO_3^{2-}]}{[HSO_3^-]}, \tag{15}$$

where $SO_2 \cdot H_2O$ is physically dissolved SO_2, HSO_3^- is the bisulfite ion, SO_3^{2-} is the sulfite ion, K_h is Henry's constant and K_1 and K_2 are the first and the second dissociation constants, respectively. Note that the Henry's and the dissociation constants are strongly dependent on temperature. In this study, we adopted the dependencies of the equilibrium constants for the above reactions K_h, K_1 and K_2 on temperature from Maahs (1982). The total concentration of the dissolved sulfur in oxidation state IV can be calculated as follows:

$$[S(IV)] = [SO_2 \cdot H_2O] + [HSO_3^-] + [SO_3^{2-}]. \tag{16}$$

Since the diffusivities of $SO_2 \cdot H_2O$, SO_3^{2-} and HSO_3^- are sufficiently close (see, e.g., Baboolal et al., 1981; Huckaby and Ray, 1989), the concentration of

S(IV) inside the droplet can be determined from Eq. (1). Concentrations of $SO_2 \cdot H_2O$, sulfite SO_3^{2-} and bisulfite HSO_3^- ions can be found by assuming that ions diffuse in such a way as to achieve local electrical neutrality which implies the balance of the electrical charges in any given location:

$$[H^+] = [OH^-] + [HSO_3^-] + 2[SO_3^{2-}] \tag{17}$$

Taking into account that the characteristic times of chemical processes and time required for establishing phase equilibrium are much less than characteristic times of molecular diffusion, we assumed local equilibrium in a liquid phase (for details, see Schwartz and Freiberg, 1981).

Using the expressions (13)–(15) for the constants K_h, K_1, K_2 and Eqs. (16) and (17) after simple algebra we can obtain the following system of algebraic equations for determining ion concentrations at any location inside the droplet:

$$\begin{aligned} &K_w + x_3 x_1 + 2x_4 x_1 - x_1^2 = 0,\\ &K_1 x_2 - x_3 x_1 = 0,\\ &K_2 x_3 - x_4 x_1 = 0,\\ &x_2 + x_3 + x_4 - [\mathrm{S(IV)}] = 0, \end{aligned} \tag{18}$$

where $x_1 = [H^+]$, $x_2 = [SO_2 \cdot H_2O]$, $x_3 = [HSO_3^-]$, $x_4 = [SO_3^{2-}]$ and K_w is the equilibrium constant of water self-ionization (Stumm and Morgan, 1981):

$$K_w = [OH^-][H^+] = \exp\left(-\frac{10294.8349}{T} + 14.0169 - 0.0392T\right)[M^2]. \tag{19}$$

The boundary condition for the equation of diffusion in a liquid phase (see Eq. (1)) reads:

$$Y_{S(IV)} = \frac{M_{S(IV)}}{\rho_L} H^*_{S(IV)} p_{SO_2}, \tag{20}$$

where $M_{S(IV)}$ is the molar mass of the absorbate, p_{SO_2} is the partial pressure of SO_2 species in the gas, and $H^*_{S(IV)}$ is the effective Henry's constant $H^*_{S(IV)} = H_{SO_2} \times [1 + K_1/[H^+] + K_1K_2/[H^+]^2]$ (see, e.g., Seinfeld, 1986). Note that H_{SO_2} is identical to Henry's constant, K_h. At the gas–liquid interface $T_e = T^{(L)}$, and at the center of the droplet symmetry condition implies that

$$\left.\frac{\partial Y_A^{(L)}}{\partial r}\right|_{r=0} = 0, \quad \left.\frac{\partial T^{(L)}}{\partial r}\right|_{r=0} = 0. \tag{21}$$

At $r \to \infty$ and $t > 0$, the "soft" boundary conditions at infinity are imposed:

$$\left.\frac{\partial T_e}{\partial r}\right|_{r\to\infty} = 0, \quad \left.\frac{\partial Y_j}{\partial r}\right|_{r\to\infty} = 0. \tag{22}$$

2.3. Numerical scheme

The presence of two computational domains ($0 \leqslant r \leqslant R(t)$ for the liquid phase, and $r \geqslant R(t)$ for the gaseous phase) for the system of Eqs. (1)–(4) which are separated by a moving boundary $r = R(t)$ complicates the numerical solution. Moreover, the characteristic times of the heat and mass transfer in the gaseous phase and heat transfer in the liquid phase are considerably smaller than the characteristic time of the diffusion of soluble component in liquid. In order to overcome these problems, we introduced the following dimensionless time variable $\tau = D_L t/R_0^2$. Then the governing equations can be rewritten for time variable τ using the following coordinate transformations (see, e.g., Ray et al., 1987): $x = 1 - r/R(t)$ in the domain $0 \leqslant r \leqslant R(t)$, and $w = \sigma^{-1}(r/R(t) - 1)$ in the domain $r \geqslant R(t)$. The parameter σ was chosen such that the concentrations of the gaseous species and the gas phase temperature attain their initial values at the distance $\sigma R(t)$. In the transformed computational domains, the coordinates $x \in [0,1]$, $w \in [0,1]$, and these domains can be treated identically in numerical calculations. The gas–liquid interface is located at $x = w = 0$. The system of nonlinear parabolic partial differential Eqs. (1)–(4) was solved using the method of lines developed by Sincovec and Madsen (1975). The spatial discretization on a three-point stencil was used in order to reduce the system of the time-dependent partial differential equations to a semi-discrete approximating system of coupled ordinary differential equations. Thus, the system of partial parabolic differential equations is approximated by a system of ordinary differential equations in time for the unknown functions T_e, $T^{(L)}$, $Y_A^{(L)}$ and Y_j at the mesh points. The mesh points were spaced adaptively using the following formula:

$$x_i = \left(\frac{i-1}{N}\right)^n, \qquad i = 1, \ldots, N+1. \tag{23}$$

Consequently, mesh points cluster near the left boundary where the gradients are steep. In Eq. (23), N is the chosen number of mesh points, n is an integer coefficient (in our calculations n is chosen equal to 3).

The resulting system of ordinary differential equations was solved using a backward differentiation method. Generally, in the numerical solution, 151 mesh points and an error tolerance $\sim 10^{-5}$ in time integration were employed. Variable time steps were used to improve the computing accuracy and efficiency. During numerical solution of the system of Eqs. (1)–(4), the properties ρ, c_p, D_j, and k_e were evaluated simultaneously at each grid point at each time step. The compilation of the formulas for calculating these properties is presented by Reid et al. (1987) and Ben-Dor et al. (2003a, b). Properties of the liquid and the gaseous phases were adopted from Reid et al. (1987). The system of nonlinear algebraic Eqs. (18) was solved at each grid point at each time step. Calculations were terminated when the condition $R/R_0 \leqslant 0.1$ was fulfilled.

3. Results and discussion

The above model of gas absorption by evaporating (growing) droplet was applied to study evaporation of water droplet immersed in a stagnant ternary gaseous mixture composed of nitrogen (N_2), soluble sulfur dioxide (SO_2), and vapor of the water droplet. Using the present model of gas absorption with subsequent dissociation reaction, we performed the numerical calculations for the dependence of average molar concentrations of aqueous sulfur compounds and the average concentration of total dissolved sulfur S(IV) in water droplet vs. time (see Figs. 1–4). The average concentration of the ith species concentration is determined as follows:

$$\langle C_i \rangle = \frac{1}{V_d} \int C_i(r) r^2 \sin\vartheta \, dr \, d\vartheta \, d\varphi, \tag{24}$$

where subscript i denotes the chemical compound such as physically absorbed sulfur dioxide $SO_2 \cdot H_2O$, sulfite SO_3^{2-} and bisulfite HSO_3^- ions. The results of calculations of aqueous sulfur species in evaporating (RH = 70%) and growing (RH = 101%) droplets with the initial radius 10 μm are presented in Figs. 1–4. In these calculations, we assumed different concentrations of SO_2 in the ambient gaseous mixture such as 0.01 ppm (Figs. 1 and 3), 0.2 ppm (Fig. 2) and 0.01 ppb (Fig. 4). The concentration of sulfur dioxide equal to 0.2 ppm is typical for highly polluted atmosphere, and the concentration of SO_2 of the order of 1 ppb is typical for clean atmosphere (see, e.g., Seinfeld, 1986). As can be seen from Figs. 1–4, the average concentration of the total dissolved sulfur [S(IV)] is significantly larger than concentration of $[SO_2 \cdot H_2O]$ in the liquid phase. Inspection of the Figs. 1–3 shows that in the case when the ambient concentration of SO_2 is in the range from 0.01 to 0.2 ppm, the ions of HSO_3^- constitute the major fraction of the total amount of tetravalent sulfur species. Similar phenomenon has

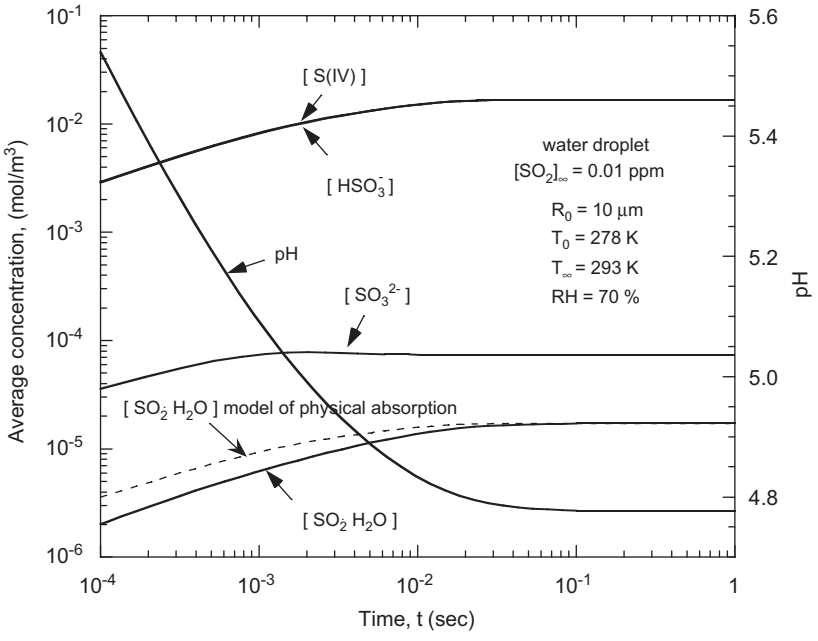

Fig. 1. Average concentration of aqueous [S(IV)], $[SO_2 \cdot H_2O]$, $[HSO_3^-]$, $[SO_3^{2-}]$ and pH vs. time (RH = 70%, $[SO_2]_\infty = 0.01$ ppm).

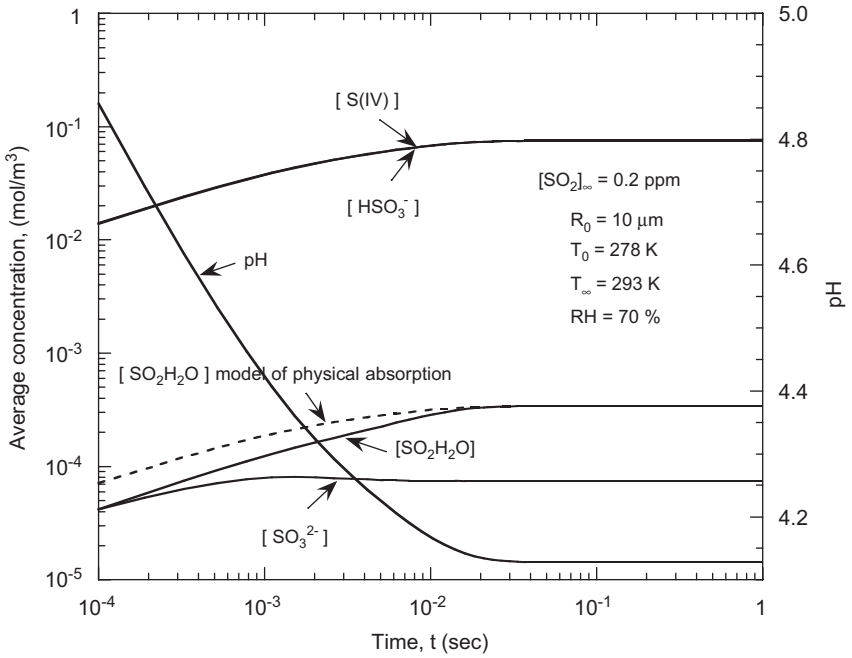

Fig. 2. Average concentration of aqueous [S(IV)], $[SO_2 \cdot H_2O]$, $[HSO_3^-]$, $[SO_3^{2-}]$ and pH vs. time (RH = 70%, $[SO_2]_\infty = 0.2$ ppm).

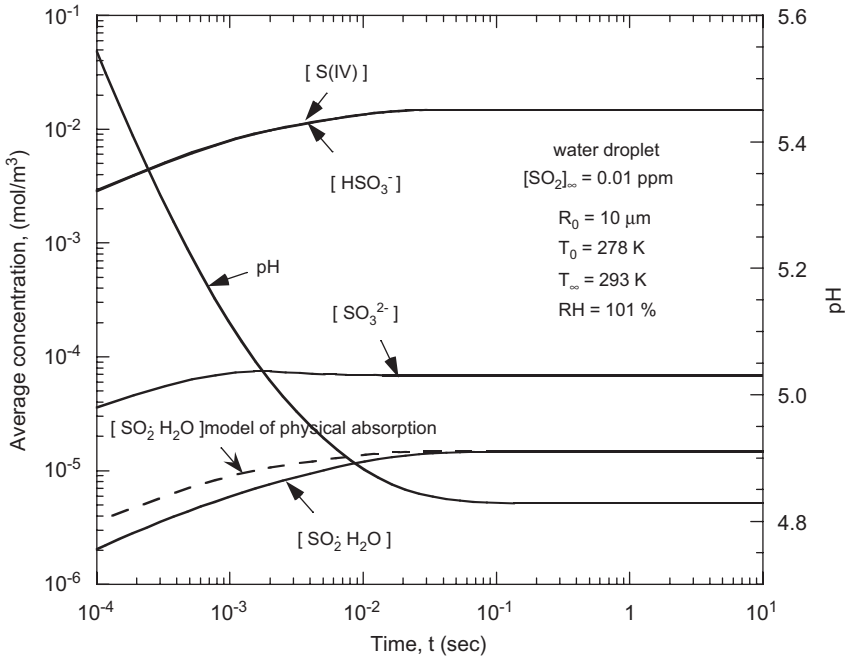

Fig. 3. Average concentration of aqueous [S(IV)], $[SO_2 \cdot H_2O]$, $[HSO_3^-]$, $[SO_3^{2-}]$ and pH vs. time (RH = 101%, $[SO_2]_\infty = 0.01$ ppm).

been found by Huckaby and Ray (1989) on a basis of the numerical calculations performed for the concentrations of SO_2 in a gaseous phase in the range from 10^{-6} to 10^{-5} mol m^{-3}. In the case of very small concentrations of SO_2 in an ambient air (of the order of 0.01 ppb) for small time elapsed from the beginning of gas absorption the contributions of HSO_3^- and SO_3^{2-} chemical compounds in the total

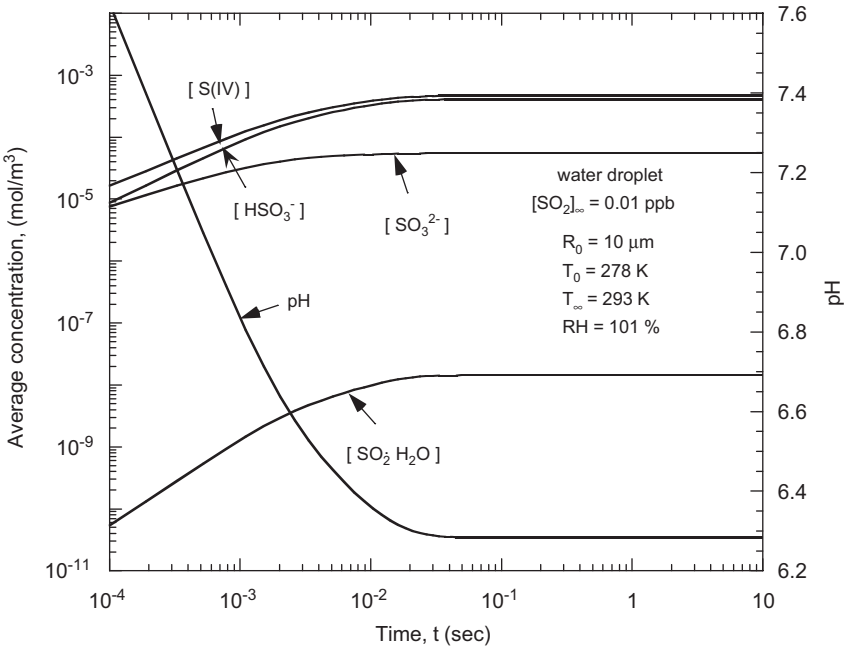

Fig. 4. Average concentration of aqueous [S(IV)], $[SO_2 \cdot H_2O]$, $[HSO_3^-]$, $[SO_3^{2-}]$ and pH vs. time (RH = 101%, $[SO_2]_\infty = 0.01$ ppb).

concentration of the dissolved sulfur [S(IV)] are comparable while for large time the contribution of HSO_3^- to the concentration of [S(IV)] is predominant (see Fig. 4).

Average concentration of $[SO_2 \cdot H_2O]$ calculated using the present model was compared with the results obtained using the model of physical absorption suggested by Elperin et al. (2007a). The comparison (see Figs. 1–3) shows that ignoring the subsequent equilibrium dissociation reactions (dashed lines) leads to overestimating average concentration of $[SO_2 \cdot H_2O]$ at the transient stage of gas absorption. As can be seen from Figs. 1–3 with an increase of concentration of SO_2 in the gaseous phase, the share of $SO_2 \cdot H_2O$ in total concentration of dissolved sulfur species [S(IV)] increases while the share of SO_3^{2-} in [S(IV)] decreases.

We also performed calculations of temporal variation of pH for evaporating and growing droplets. As can be seen from Figs. 1 and 3, the magnitude of pH is larger for growing droplets.

The dependence of the ratio $pH_{sat}/pH_{0,sat}$ at the stage of saturation vs. relative humidity (RH) is shown in Fig. 5, where pH_0 denotes the value of pH calculated for the relative humidity 0% at the stage of saturation. The calculations were performed for different values of ambient concentration of sulfur dioxide (0.01 and 0.2 ppm). The ambient temperature was assumed to be equal to 293 K. Calculations were

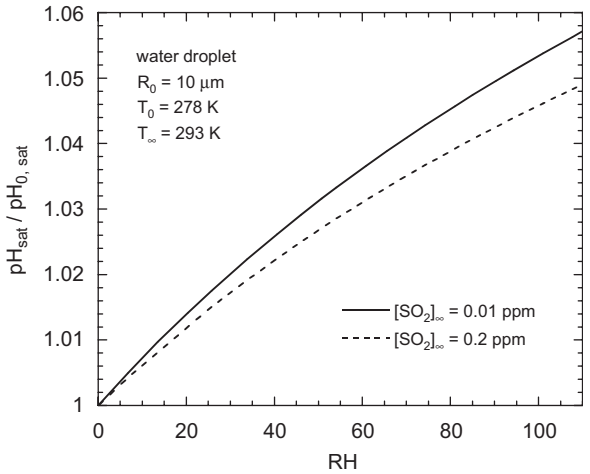

Fig. 5. Dependence of related value of pH ($pH_{sat}/pH_{0,sat}$) vs. RH.

performed for the droplet with the initial radius 10 μm. Inspection of Fig. 5 shows that the value of pH at the saturation stage is higher for lower concentration of sulfur dioxide in the gaseous phase. As can be seen from Fig. 5 the ratio $pH_{sat}/pH_{0,sat}$ increases with the increase of the relative humidity (RH). The main factors leading to pH increase with the increase of RH are the rise of the droplet temperature and increasing dilution of H^+ ions. Droplet temperature rise causes the reduction of

saturation concentration of H^+ ions, while RH increase leads to either slowing droplet evaporation or to droplet growth due to condensation. Consequently, dilution of H^+ ions increases with the increase of humidity. All these trends are valid for concentrations of all ions in a droplet (see Fig. 6).

Henry's law constant as well as the effective Henry's law constant and, consequently, concentration of the dissolved species inside the droplet strongly depend on temperature. Therefore, droplet surface temperature is one of the most important parameters for investigating gas absorption by evaporating/growing droplets. Comparison of the results obtained using the model of physical absorption of sulfur dioxide in water droplet with the predictions of the model taking into account the subsequent equilibrium dissociation reactions shows that the model of physical absorption underestimates the droplet surface temperature (Fig. 7). Calculations were performed for a water droplet with the initial radius 25 μm evaporating in dry N_2/SO_2 gaseous mixture. The mass fraction of SO_2 in ambient gaseous mixture is 0.5. The calculations were performed for ambient temperature 288 K.

Higher values of droplets surface temperature predicted by the model of gas absorption with dissociation of the dissolved gas are the result of the enhanced thermal effect of absorption. The enhanced thermal effect of absorption with dissociation is caused by the increase of the total amount of the absorbed gas due to larger value of the effective Henry's constant.

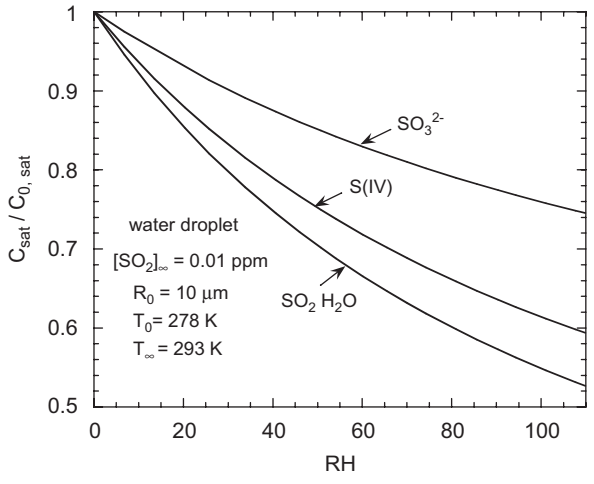

Fig. 6. Dependence of the normalized concentration of saturation of different ions in a droplet vs. RH.

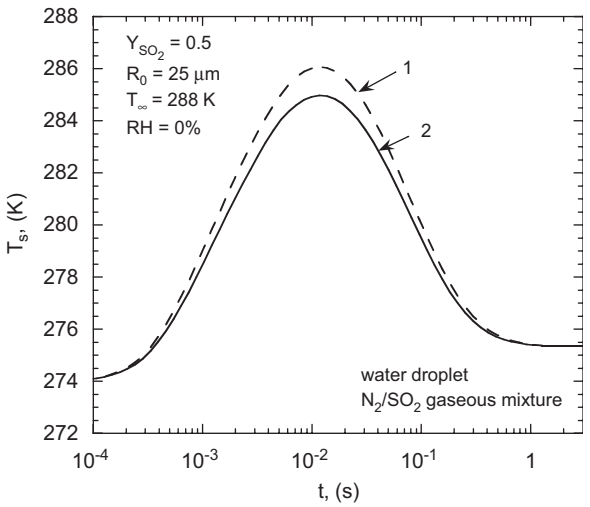

Fig. 7. Droplet surface temperature as a function of time for a water droplet evaporating in $N_2/SO_2/H_2O$ gaseous mixture: (1) model taking into account the equilibrium dissociation reactions and (2) model of physical absorption.

The maximum of droplet surface temperature during the transient period of evaporation in an air–water vapor–soluble gas mixture occurs due to competition of different phenomena which lead to cooling and heating of droplet surface simultaneously (see Fig. 7). Evaporation leads to droplets surface temperature decrease while at the same time thermal effect of dissolution increases droplet surface temperature. Interaction of these effects results in a maximum of droplets surface temperature. At the stage of gas absorption thermal effect of dissolution is dominant, and droplet surface temperature increases. When gas absorption and heating slow down, cooling due to evaporation prevails. In the framework of the model of physical absorption the nonlinear behavior of the droplet surface temperature was discussed by Elperin et al. (2007a). The detailed scheme of the interrelation between heat and mass transport during transient period of droplet evaporation with gas absorption is shown in Fig. 8. The scheme takes into account subsequent aqueous-phase equilibrium dissociation reactions. Numerical analysis showed that in the case of small concentrations of SO_2 in a gaseous phase the effects of Stefan flow and heat of absorption on the droplet surface temperature can be neglected.

4. Conclusions

In this study, we developed a numerical model of simultaneous heat and mass transfer during evaporation and vapor condensation on the surface

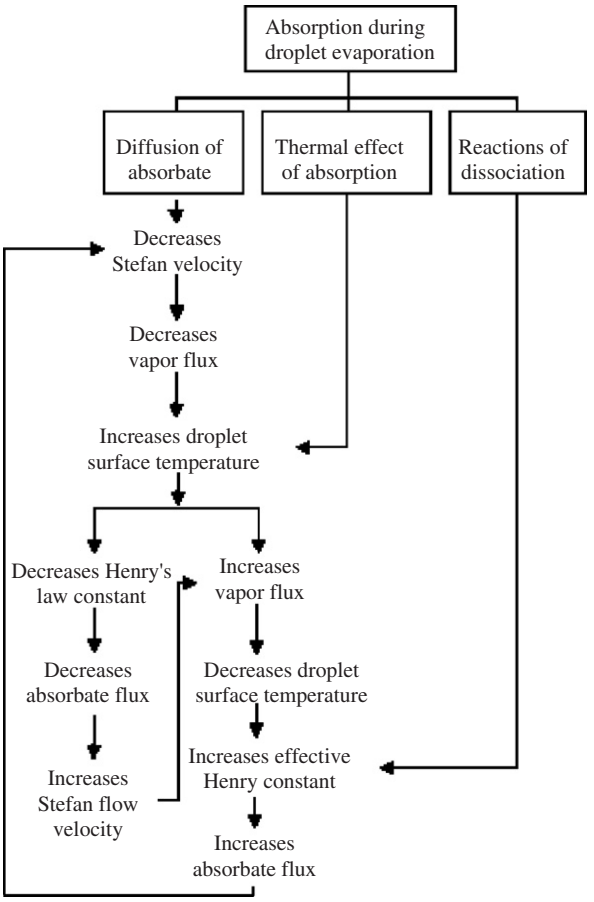

Fig. 8. Schematic description of the interrelation between heat and mass transport during the transient period of droplet evaporation with gas absorption.

of a stagnant droplet in the presence of inert admixtures containing non-condensable soluble gas. It is assumed that gas absorption is accompanied by subsequent aqueous-phase equilibrium dissociation reaction.

The developed model was compared with the model of physical absorption of soluble gas in water droplet. The results obtained in this study allow us to draw the following conclusions:

1. Heat and mass transfer rates in water droplet–air–water vapor system at short times are considerably enhanced under the effects of Stefan flow, heat of absorption and dissociation reactions within the droplet.
2. Comparison of the results predicted by the model of physical absorption of sulfur dioxide in water droplet with the model that takes into account the subsequent equilibrium dissociation reactions showed that the model of physical absorption underestimates the droplet surface temperature and overestimates the average concentration of $[SO_2 \cdot H_2O]$ at the transient stage of gas absorption.
3. With an increase of concentration of SO_2 in a gaseous phase, the share of $SO_2 \cdot H_2O$ in the total concentration of the dissolved sulfur species [S(IV)] increases while the share of SO_3^{2-} in [S(IV)] decreases.
4. Magnitude of pH in a droplet at the saturation stage is higher for lower concentration of sulfur dioxide in a gaseous phase.
5. The developed model allows us to calculate the value of pH vs. time for evaporating and growing droplets. The performed calculations showed that pH increases with the increase of the relative humidity (RH). The main factors leading to pH increase with the increase of RH are the rise of the droplet temperature and increasing dilution of H^+ ions.
6. Non-monotonic dependence of droplet surface temperature vs. time stems from the interaction of different phenomena. In particular, thermal effect of solubility and Stefan flow result in the maximum of the droplet surface temperature during the transient period of droplet evaporation. Numerical analysis showed that in the case of small concentrations of SO_2 in the gaseous phase the effects of Stefan flow and heat of absorption on the droplet surface temperature can be neglected.
7. Even for small concentrations of soluble species only taking into account mutual influence of absorption and condensation (evaporation) allows correct prediction of the influence of condensation (evaporation) on gas absorption. The reason is the nonlinearity of heat and mass transfer equations describing gas absorption and droplet evaporation (growth) and the nonlinear dependence of chemical equilibrium constants on temperature.

The performed analysis of gas absorption by liquid droplets accompanied by droplets evaporation and vapor condensation on the surface of liquid droplets can be used in calculations of scavenging of hazardous gases in atmosphere by rain and atmospheric cloud evolution.

References

Alexandrova, S., Marion, M., Lepinasse, E., Saboni, A., 2004. Mass transfer modeling of SO_2 into large drops. Chemical Engineering and Technology 27, 676–680.

Baboolal, L.B., Pruppacher, H.R., Topalian, J.H., 1981. A sensitivity study of a theoretical model of SO_2 scavenging by water drops in air. Journal of the Atmospheric Sciences 38, 856–870.

Ben-Dor, G., Elperin, T., Krasovitov, B., 2003a. Numerical analysis of temperature and concentration jumps on transient evaporation of moderately large ($0.01 \lesssim Kn \lesssim 0.3$) droplets in non-isothermal multicomponent gaseous mixtures. Heat and Mass Transfer 39, 157–166.

Ben-Dor, G., Elperin, T., Krasovitov, B., 2003b. Effect of thermo- and diffusiophoretic motion of flame-generated particles in the neighbourhood of burning droplets in microgravity conditions. Proceedings of the Royal Society London A 459, 677–703.

Elperin, T., Fominykh, A., 2005. Conjugate mass transfer during gas absorption by falling liquid droplet with internal circulation. Atmospheric Environment 39, 4575–4582.

Elperin, T., Fominykh, A., Krasovitov, B., 2007a. Evaporation and condensation of large droplets in the presence of inert admixtures containing soluble gas. Journal of the Atmospheric Sciences 64, 983–995.

Elperin, T., Fominykh, A., Orenbakh, Z., 2007b. Coupled heat and mass transfer during nonisothermal absorption by falling droplet with internal circulation. International Journal of Refrigeration 30, 274–281.

Flossmann, A.I., 1998. Clouds and pollution. Pure and Applied Chemistry 70, 1345–1352.

Gardner, J.A., Watson, L.R., Adewuyi, Y.G., Davidovits, P., Zahniser, M.S., Worsnop, D.R., Kolb, C.E., 1987. Measurement of the mass accommodation coefficient of SO_2(g) on water droplets. Journal of Geophysical Research—Atmospheres 92 (D9), 10887–10895.

Huckaby, J.L., Ray, A.K., 1989. Absorption of sulfur dioxide by growing and evaporating water droplets. Chemical Engineering Science 44, 2797–2808.

Maahs, H.G., 1982. Sulfur dioxide/water equilibria between 0° and 50 °C. An examination of data at low concentrations. In: Schryer, D.R. (Ed.), Heterogeneous Atmospheric Chemistry. American Geophysical Union, pp. 187–195.

Marion, M., Lépinasse, E., Saboni, A., 2006. SO_2 absorption and desorption by an accelerating water droplet undergoing vaporization. International Journal of Heat and Fluid Flow 27, 290–297.

Mitra, S.K., Hannemann, A.U., 1993. On the scavenging of SO_2 by large and small rain drops. V. A wind-tunnel and theoretical study of the desorption of SO_2 from water drops containing S(IV). Journal of Atmospheric Chemistry 16, 201–218.

Pruppacher, H.R., Klett, J.D., 1997. Microphysics of Clouds and Precipitation, second ed. Kluwer Academic Publishers, Dordrecht.

Ray, A.K., Huckaby, J.L., Shah, T., 1987. Thermal effects of condensation on absorption of gases in growing droplets. Chemical Engineering Science 42, 1955–1967.

Reid, R.C., Prausnitz, J.M., Poling, B.E., 1987. The Properties of Gases and Liquids, fourth ed. McGraw-Hill, NY.

Saboni, A., Alexandrova, S., 2001. Sulfur dioxide absorption by water drops. Chemical Engineering Journal 84, 577–580.

Schwartz, S.E., Freiberg, J.E., 1981. Mass-transport limitation to the rate of reaction of gases in liquid droplets—application to oxidation of SO_2 in aqueous solutions. Atmospheric Environment 15, 1129–1144.

Seinfeld, J.H., 1986. Atmospheric Chemistry and Physics of Air Pollution. Wiley, NY.

Sincovec, R.F., Madsen, N.K., 1975. Software for nonlinear partial differential equations. ACM Transactions on Mathematical Software 1, 232–260.

Stumm, W., Morgan, J.J., 1981. Aquatic Chemistry—An Introduction Emphasizing Chemical Equilibria in Natural Waters, second ed. Wiley-Interscience, NY, p. 127.

Walcek, C.J., Pruppacher, H.R., 1984. On the scavenging of SO_2, by cloud and raindrops: I. A theoretical study of SO_2, absorption and desorption for water drops in air. Journal of Atmospheric Chemistry 1, 269–289.

Walcek, C.J., Pruppacher, H.R., Topalian, J.H., Mitra, S.K., 1984. On the scavenging of SO_2 by cloud and rain drops. II: An experimental study of SO_2 absorption and desorption by water drops in air. Journal of Atmospheric Chemistry 1, 291–306.

Waltrop, A., Mitra, S.K., Flossmann, A.I., Pruppacher, H.R., 1991. On the scavenging of SO_2 by cloud and rain drops. 4. A wind-tunnel and theoretical study of the absorption of SO_2 in the ppb(v) range by water drops in the presence of H_2O_2. Journal of Atmospheric Chemistry 12, 1–17.